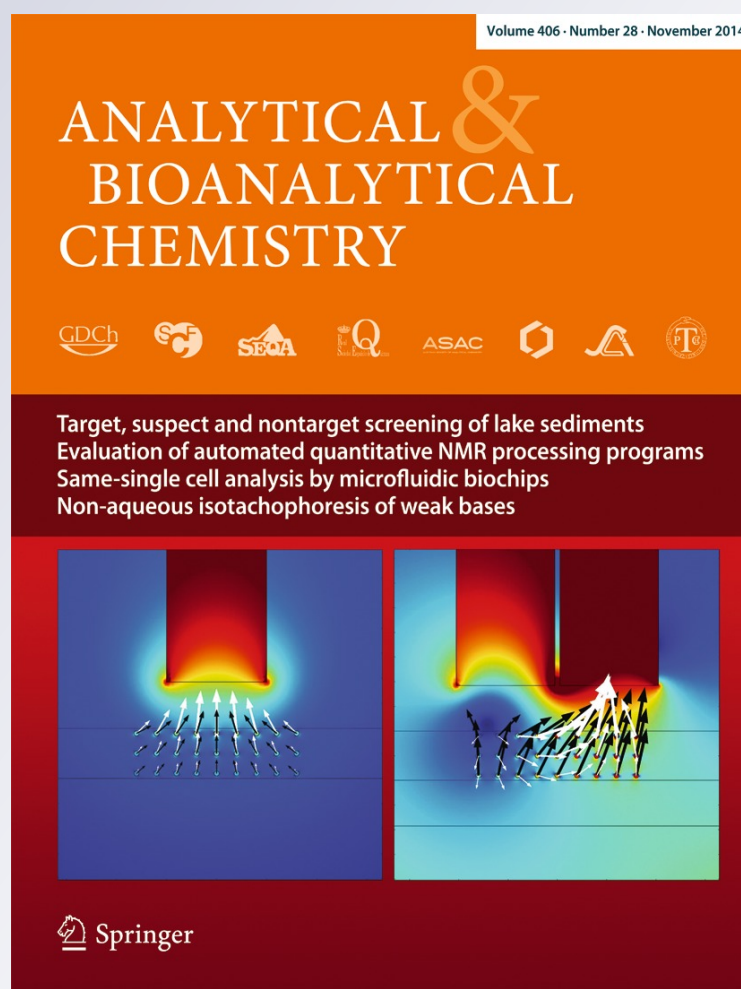*Same-single-cell analysis using the microfluidic biochip to reveal drug accumulation enhancement by an amphiphilic diblock copolymer drug formulation*

Avid Khamenehfar, Chung Ping Leon Wan, Paul C. H. Li, Kevin Letchford & Helen M. Burt

Springer

Springer

RESEARCH PAPER

Same-single-cell analysis using the microfluidic biochip to reveal drug accumulation enhancement by an amphiphilic diblock copolymer drug formulation

Avid Khamenehfar · Chung Ping Leon Wan ·
Paul C. H. Li · Kevin Letchford · Helen M. Burt

Abstract Multidrug resistance (MDR) is one of the major obstacles in drug delivery, and it is usually responsible for unsuccessful cancer treatment. MDR may be overcome by using MDR inhibitors. Among different classes of these inhibitors that block drug efflux mediated by permeability-glycoprotein (P-gp), less toxic amphiphilic diblock copolymers composed of methoxypolyethyleneglycol-block-polycaprolactone (MePEG-b-PCL) have been studied extensively. The purpose of this work is to evaluate how these copolymer molecules can reduce the efflux, thereby enhancing the accumulation of P-gp substrates (e.g., daunorubicin or DNR) in MDR cells. Using conventional methods, it was found that the low-molecular-weight diblock copolymer, $\text{MePEG}_{17}\text{-b-PCL}_5$ (PCL5), enhanced drug accumulation in MDCKII-MDR1 cells, but the high-molecular-weight version, $\text{MePEG}_{114}\text{-b-PCL}_{200}$ (PCL200), did not. However, when PCL200 was mixed with PCL5 (and DNR) in order to encapsulate them to facilitate drug delivery, there was no drug enhancement effect attributable to PCL5, and the reason for this negative result was unclear. Since drug accumulation measured on different cell batches originated from single cells, we employed the same-single-cell analysis in the accumulation mode (*SASCA-A*) to find out the reason. A microfluidic biochip was used to select single MDR cells, and the accumulation of DNR was fluorescently measured in real time on these cells in the absence and presence of PCL5. The *SASCA-A* method allowed us to obtain drug accumulation information faster in comparison to conventional assays. The *SASCA-A* results, and subsequent curve-fitting analysis of the data, have confirmed that when PCL5 was encapsulated in PCL200 nanoparticles as soon as they were synthesized, the ability of PCL5 to enhance DNR accumulation was retained, thus suggesting PCL200 as a promising delivery system for encapsulating P-gp inhibitors, such as PCL5.

Keywords Same-single-cell analysis · Multidrug resistance · Microchip · Amphiphilic diblock copolymer

Abbreviations

CsA	Cyclosporine A
DMEM	Dulbecco's modified Eagle's medium
DMSO	Dimethyl sulfoxide
DNR	Daunorubicin
DOX	Doxurubicin
FBS	Fetal bovine serum
HBSS	Hanks' balanced salt solution
MDCK	Madin-Darby canine kidney
MDR	Multidrug resistance
MePEG-b-PCL	Methoxypolyethyleneglycol-block-polycaprolactone
MTS	3-(4,5-Dimethylthiazol-2-yl)-5-(3-carboxymethoxyphenyl)-2-(4-sulfophenyl)-2H-tetrazolium
SASCA-A	Same single cell analysis in the drug accumulation mode
PBS	Phosphate buffered saline
PCL5	$\text{MePEG}_{17}\text{-b-PCL}_5$
PCL200	$\text{MePEG}_{114}\text{-b-PCL}_{200}$
PEN/STR	Penicillin/streptomycin

A. Khamenehfar · P. C. H. Li (✉)
Department of Chemistry, Simon Fraser University, 8888 University Drive, Burnaby, BC V5A 1S6, Canada
e-mail: paulli@sfu.ca

C. P. L. Wan · K. Letchford · H. M. Burt
Faculty of Pharmaceutical Sciences, The University of British Columbia, 2146 East Mall, Vancouver, BC V6T 1Z3, Canada

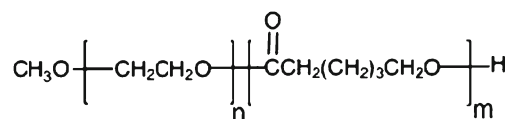| P-gp | Permeability-glycoprotein |
| SD | Standard deviation |
| Tryp/EDTA | Trypsin-ethylenediaminetetraacetic acid |

Fig. 1 Structure of (MePEG$_n$-b-PCL$_m$) diblock copolymer; n: number of ethyleneglycol repeat units; m: number of caprolactone repeat units

Introduction

Permeability-glycoprotein (P-gp), a 170-kDa transmembrane drug transporter protein, plays a major role in cellular multi-drug resistance (MDR) via the efflux of different classes of chemotherapeutic agents or drugs such as anthracyclines, taxanes, vinca alkaloids, and camptothecins. This drug efflux unfortunately reduces the effectiveness of chemotherapy [1, 2]. Since the discovery of P-gp, the development of P-gp inhibitors, among other drug transporter inhibitors, has drawn a great deal of attention, and a number of agents with the P-gp inhibitory activity have been identified. For instance, verapamil and cyclosporine A (CsA), typically inhibiting P-gp by binding to its drug-binding domain [3–5], were found to enhance the accumulation of P-gp substrates in cancer cells. However, very few of these inhibitors have shown substantial clinical benefits, mainly because of the toxicity of these inhibitory compounds [4, 6].

In recent years, significant attention has been paid to the use of less toxic compounds, such as pharmaceutical excipients, to act as P-gp inhibitors [7]. These compounds, such as polysorbates (i.e., Tween 20, polysorbate 80), Triton X-100, Cremophor EL, Pluronic P85, Peceol, Gelucire 44/14, Labrasol, and tocopheryl polyethylene glycol succinate (TPGS), have been demonstrated to enhance the cellular accumulation of P-gp substrates [8–15]. In the last decade, Burt's group has conducted extensive work to develop the pharmaceutical excipients as biocompatible P-gp inhibitors based on methoxypolyethyleneglycol-block-polycaprolactone [16–19]. These are diblock copolymers composed of a hydrophobic block (i.e., polycaprolactone or PCL) that binds via an ester linkage to a hydrophilic block (i.e., polyethylene glycol or PEG). These diblock copolymers are abbreviated as MePEG$_n$-b-PCL$_m$, where m and n are the number of repeat units of caprolactone and ethylene glycol, respectively (Fig. 1) [12, 16]. Burt et al. reported MePEG$_{17}$-b-PCL$_5$ (abbreviated as PCL5) diblock copolymer as a novel P-gp inhibitor of less toxicity, and it enhanced the cellular accumulation of P-gp substrates including rhodamine-123, rhodamine-6G, paclitaxel, and doxorubicin [16–20]. Furthermore, PCL5 has been reported to solubilize hydrophobic anti-cancer drugs (such as paclitaxel) within the PCL5 micelles and deliver drugs to various tumor sites [12, 17, 21].

More recently, Letchford et al. formulated the high-molecular-weight copolymer, MePEG$_{114}$-b-PCL$_{200}$, as

the carrier to encapsulate both PCL5 and a chemotherapeutic drug so that they can be co-delivered to MDR cancer cells [22]. In the mixed molecular weight copolymer (PCL200/5), PCL5 was co-encapsulated with taxanes in a drug delivery system made of MePEG$_{114}$-b-PCL$_{200}$ (PCL200) copolymers. This drug formulation was found to be effective in overcoming MDR in Madin-Darby canine kidney (MDCKII-MDR1) cells that over-express P-gp. Although the use of PCL200/5 nanoparticles has been found to be a promising system for delivering the drug payload and overcoming MDR, the actual mechanism of how this system inhibits P-gp remains unclear.

In cellular analysis applications, single-cell analysis can provide information on cell-to-cell variations, and so this method is preferred over the traditional bulk cellular analysis [23, 24]. Additionally, the physicochemical modeling of biological processes demands that the data are obtained from a single cell [25]. Recently, the microfluidic chip, with dimensions of internal structures compatible with single cells, has become a powerful tool for single cell analysis, including the advantages of low reagent consumption (μL), low cost, and low sample requirement (100–1000 cells) [26, 27]. Li's group developed the same single cell analysis (SASCA-A) method to fluorescently measure intracellular drug accumulation [27]. In contrast to conventional methods (i.e., radiochemical method), SASCA-A can provide real-time data of the accumulation of a drug (i.e., daunorubicin or DNR) in an individual cell. The real-time increase in fluorescent intensity of a single MDR cell directly indicates an accumulation of DNR, and this increase eventually reaches a plateau because of drug efflux mediated by P-gp in the MDR cell. Upon co-application of a P-gp inhibitor with DNR, the further increase in fluorescent intensity of DNR is the result of the enhancement of drug accumulation due to the inhibitor; this phenomenon is called MDR reversal. To better understand the cellular drug accumulation process, a mathematical model is required to study the kinetics of drug accumulation and of its enhancement on a single MDR cell, and the SASCA-A measurement provides real-time data for us to conduct curve fitting to the data. In this way, we compared the DNR accumulation kinetics when PCL5 and DNR were either encapsulated or un-encapsulated in PCL200 to find out whether PCL200-encapsulated PCL5 demonstrates the same P-gp inhibitory function as un-encapsulated PCL5.

Materials and methods

Microchip design

The layout of the microfluidic glass chip (1.5 cm×2.7 cm) consists of four channels, four reservoirs, and one chamber containing the cell retention structure (Fig. 2). The right and left reservoirs (3, 4) serve as the inlet and waste reservoirs, respectively; whereas, the top reservoirs (1, 2) are used for drug delivery. The channel depth was 40 μm, whereas the reservoirs were 0.6 mm deep and 2 mm in diameter.

The microfluidic chip was fabricated by the standard micromachining technology on glass by CMC Microsystems (Kingston, ON, Canada) as shown in Figure S1 in the Electronic Supplementary Material (ESM). Briefly, these procedures include standard chip cleaning, thin film deposition, photolithography, photoresist development, HF wet etching, reservoir forming, and chip bonding, as previously described [25, 28].

The cell retention structure located inside the chamber was used to select and retain a single cell. Based on this active cell trapping strategy, we were able to select and retain a cell in good condition and flush away any undesired cells or debris. In our microchip, the reagents flow from reservoirs 1 and 2 through the cell retention structure to the inlet and waste reservoirs (3 and 4). The flow of reagent solutions from reservoirs through the cell retention structure was modeled as described elsewhere [29]. Based on the modeled flow, there was a small zero speed point (ZSP) where the cell was trapped. Since this location was smaller than the cell size, the reagent was still able to pass by and reach the cell.

Reagents

Daunorubicin (DNR) and cyclosporine A (CsA) were obtained from Sigma-Aldrich (St. Louis, MO, USA). Dulbecco's modified Eagle's medium (DMEM), trypsin-ethylenediaminetetraacetic acid (Trypsin-EDTA) (0.025 %), penicillin/streptomycin (PEN/STR), and fetal bovine serum (FBS) were obtained from Life Technologies (Grand Island, NY, USA). Hanks' balanced salt solution (HBSS) was from Invitrogen (Grand Island, NY, USA). DNR was dissolved in DMSO (Sigma-Aldrich) to make stock solutions of 350 μM. CsA was dissolved in DMSO (Sigma-Aldrich) to make stock solutions of 500 μM. All MePEG-b-PCL amphiphilic diblock copolymers, as described in the diblock copolymers synthesis section, were diluted in HBSS at 37 °C to make stock solutions of 1 % w/v.

The MTS (3-[4,5-dimethylthiazol-2-yl]-5-[3-carboxymethoxyphenyl]-2-[4-sulfophenyl]-2H-tetrazolium) cell-proliferation assay kit was obtained from Promega (Madison, WI, USA).

Fig. 2 The microfluidic chip. (**a**) and (**b**) Images (top and side view) of the microchip (1.5 cm× 2.7 cm) filled with a blue food dye. A Canadian quarter (25 cents) was placed next to the chip for size comparison. (**c**) The chip was mounted on a heated microscope stage to maintain the physiological temperature at 37 °C. (**d**) Layout of the microfluidic device shows reservoirs 1 and 2 used for drug delivery; reservoirs 3 and 4 served as the cell inlet and waste, respectively. (**e**) The image shows the cell retention structure inside the chip that is used to trap a single cell. (**f**) and (**g**) The MDR cell retained within the cell retention structure was shown. The chip is shuttled (**f**) into and (**g**) out of the detection window (red box) to measure signal from the cell and background, respectively
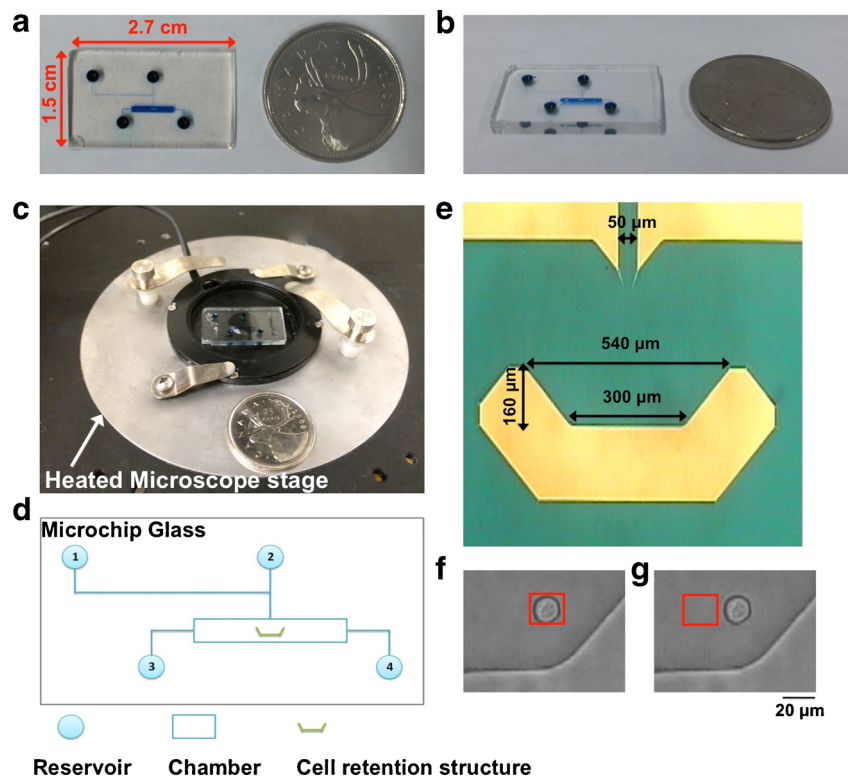
Cell culture

MDCKII and MDCKII-MDR1 cells were gifts from the National Cancer Institute, The Netherlands. Both cell lines were grown for 3–4 d in DMEM supplemented with 10 % FBS and 1 % PEN/STR. For the cell subculture, the adherent cells were detached using trypsin-EDTA and re-seeded. The MDCKII-MRDR1 cells, transfected with the human MDR1 gene [30–35], are commonly employed as quick assessment models to estimate permeability of new drug candidates, which are substrates or inhibitors of P-gp efflux pumps. We have used cells up to 17 passages. It was reported that a maximum of 25 passages have been used to monitor P-gp expression level in MDCKII-MDR cells without observing any difference in P-gp expression of cells from different passage numbers [16].

Synthesis and characterization of MePEG-b-PCL diblock copolymers

The amphiphilic diblock copolymers were composed of methoxy-terminated poly (ethylene glycol) (MePEG) and poly (caprolactone) (see Fig. 1), and they were synthesized as previously described [16, 17]. Briefly, for PCL5, MePEG with a molecular weight of 750 g/mol was mixed with ε-caprolactone in the weight ratio of 60:40 with a total mass of 50 g. For PCL200, MePEG with a molecular weight of 5000 g/mol was combined with ε-caprolactone in the weight ratio of 82:18 with a total mass of 50 g. The reactants were reacted at 140 °C for 4 h (PCL5) or for 24 h (PCL200) in a sealed round-bottomed flask containing 35 mL of anhydrous toluene, and 0.15 mL of stannous octoate was used as a catalyst. The products were purified by dissolving them in chloroform followed by precipitation with a 70/30 mix of hexane and diethyl ether. PCL5, with a short PCL block length, exists in the form of micelles, whereas PCL200 is of a higher molecular weight, existing in the form of nanoparticles.

Using gel permeation chromatography (GPC), the molecular weights and molecular weight polydispersity indexes of these copolymers were determined. The compositions of the copolymers were determined by proton NMR spectra of 10 % w/v solutions of the copolymers in chloroform, obtained from a 400 MHz Bruker Advance II + spectrometer (Bruker Corporation, Milton, ON, Canada). The degree of polymerization of copolymers was calculated using peaks situated around 1.3 and 1.55 ppm from the caprolactone methylene protons and the peaks at 3.55 ppm from the MePEG methylene protons.

On-chip drug accumulation study on single MDCKII cells

A single cell was selected from within a microfluidic biochip for SASCA-A measurements, as previously described [23, 36].

Briefly, after several cells were introduced from reservoir 3 (inlet reservoir), solutions from all other reservoirs were removed; therefore, the cells flowed from left to right inside the chamber. The desired cell moved further and passed the entrance of the cell retention structure. By adjusting the liquid levels of reservoirs 3 and 4, the cell moved back to the entrance of cell retention. Thus, the cell was pushed into the cell retention structure by inducing flow via reservoirs 1 and 2, which were connected to central reagent channel (Fig. 2d). The trapped cell (Fig. 2f) was settled for ~15 min before the fluorescence measurement started. The biochip was mounted on a heated microscope stage to maintain the analysis temperature at 37 °C (Fig. 2c), for fluorescent measurement and live cell imaging simultaneously. The serum protein in the cell medium coated the microchip surface before the cells were admitted into the chip. This strategy also helps keep the cell stationary during the SASCA-A experiment. From previous studies [16, 31], the experiments on MDCKII cells were also performed in HBSS, which contained no protein, and similar results of drug accumulation enhancement were obtained as to what we obtained in SASCA-A experiments. We believe the serum proteins do not affect the drug uptake by the MDCKII cells.

For the SASCA-A experiment, the first step was to measure the accumulation of the anticancer drug (i.e., daunorubicin or DNR) in the MDR single cell biochip in the absence of the P-gp inhibitor. In the next step, in the same cell, DNR accumulation was measured in the presence of an MDR inhibitor compound [23]. Adding MDR inhibitors increased DNR accumulation, and then the single cell fluorescence intensity was enhanced. DNR was first used for drug accumulation measurement since it was a substrate of the P-gp, and the drug also has inherent fluorescence (λ_{ex}=470 nm; λ_{em}=585 nm). The excitation light was provided by the xenon arc lamp, which was not critical to provide an impact on the cell membrane permeability.

During data collection, the chip was moved back and forth across the detection aperture window (depicted by red square in Fig. 2f and g: briefly, when the cell was inside the detection window, the cellular fluorescence was measured, whereas the background signal was measured when the cell was outside the detection window [28, 37]. Subtraction of the background from the cell signal intensity gave a corrected signal representing the drug concentration inside the cell.

The experiments were first conducted on the MDCKII cells, followed by the MDCKII-MDR1 cells. It has been reported that MDCKII-MDR1 cells have expressed efflux transporters such as P-gp [30, 38], whereas the MDCKII cell line (wild type) was used as the negative control since it has been reported not to express P-gp [17]. In the experiments, the single cell was first treated with the anticancer drug (35 μM of DNR) in the absence of MDR inhibitors (~1000 s) for drug

accumulation (control experiment). In the next step, in the same single cell, the enhanced drug accumulation was measured in the presence of a P-gp inhibitor at different concentrations (~1000 s for each step). Low-molecular-weight diblock copolymer (PCL5) was evaluated at different concentrations (0.02 %, 0.05 %, 0.10 % w/v) for its ability to inhibit the P-gp function in MDR cells. Subsequently, PCL200-encapsulated PCL5 was evaluated in a similar manner. Cyclosporine A, a well-known P-gp inhibitor [39], was used as the positive control.

Cytotoxicity of Daunorubicin and MePEG-b-PCL diblock copolymers

Cytotoxicity studies of DNR in the presence or absence of PCL5 and PCL200/5 were performed on the MDCKII and MDCKII-MDR1 cell lines. These cells were seeded at a density of 5000 cells per well in 96-well plates, and allowed to proliferate overnight (5 % CO$_2$; 95 % humidity at 37 °C) before DNR treatment. Thereafter, the culture medium comprising DMEM supplemented with 10 % FBS and 1 % PEN/STREP was removed and replaced with treatment samples containing varying concentrations of DNR (6.3 nM–0.8 μM) dissolved in the culture medium. Drug incubation was performed over a period of 3 d and cell viability was then measured using the 3-(4,5-dimethylthiazol-2-yl)-5-(3-carboxymethoxyphenyl)-2-(4-sulfophenyl)-2H-tetrazolium (MTS) cytotoxicity assay kit according to the manufacturer's instructions [16]. In experiments carried out in the presence of PCL5 and PCL 200/5, they were first dissolved in the culture medium (20-min incubation at 37 °C with warm culture medium, followed by 10-s vortexing) prior to the addition of DNR from the stock solution to make treatment samples. Cell viability is expressed as a fraction of the absorbance of samples (cells grown in treated samples) over the absorbance of the control (cells grown in the culture medium alone), both with background correction. Six wells were read per treatment, and the experiments on the plates were repeated three times.

Statistical analysis

Data are presented as the mean ± SD (standard deviation). The statistical significance test was performed by using the *t*-test.

Results and discussion

A single MDCKII cell (wild type) was first captured for measurement and signal optimization. Since the cell was non-MDR, it resulted in substantial drug accumulation. Different DNR concentrations (7, 14, 35, 70, and 350 μM) were tested in order to obtain a reasonable initial drug accumulation

signal on the cell, resulting in the initial signals of 215, 312, 715, 1040, 838 counts per second (cps), respectively. The initial signal obtained from 35 μM of DNR revealed sufficient fluorescence. This concentration, which was higher than the IC50 value of DNR, was found not to be detrimental to the cell during the experiment for ~5000 s, since the experiments were conducted in a shorter time period than the conventional 72-h cytotoxicity assay. Therefore, subsequent experiments were carried out with 35 μM of DNR.

Drug accumulation on a MDR cell: background correction/data normalization

After the DNR concentration was optimized, drug accumulation on single cells was evaluated in the absence and presence of MDR inhibitors such as PCL5 and CsA. The same single cell analysis in the accumulation mode (*SASCA-A*) was adopted and the data analysis was conducted after background correction. As shown in Fig. 3a, the original raw data depicts DNR accumulation on a single MDCKII-MDR1 cell in the presence of 35 μM of DNR for 1000 s. The spikes were the results of the measurement: the high level represents the signal of the cell plus the background, and the low level illustrates the fluorescence signal of the background. As shown in Fig. 3b, the background correction was applied so that the low-level became zero. Figure 3b shows the corrected cell fluorescence intensity (denoted as F_i) given as follow:

$$F_i = F_t - F_b \tag{1}$$

where F_t and F_b are total DNR fluorescence intensity and background level, respectively.

The spikes were removed in order to do curve fitting analysis because only the top-level data points were needed. Thereafter, the signals were normalized by dividing F_i by the initial values of DNR outside the cell (depicted as F_e in Fig. 3a). The normalized parameter (denoted as F_n) was given as follow:

$$F_n = \frac{F_i}{F_e} \tag{2}$$

where F_i and F_e represent intracellular and extracellular DNR fluorescence intensity, respectively. Since the MDR cell had drug efflux concurrent with drug uptake, it took a short time for the drug accumulation curve to reach a plateau.

Effect of MePEG$_{17}$-b –PCL$_5$ (PCL5) on DNR accumulation

SASCA-A experiments were conducted on single MDCKII-MDR1 cells to evaluate the MDR reversal effect of PCL5. A typical experimental result is shown in Fig. 4a. Although the initial drug accumulation due to DNR in the absence of PCL5 was low, an obvious slope change in the curve or enhancement

Fig. 3 Drug accumulation on a single MDCKII-MDR1 cell, the background correction and data normalization. (**a**) Raw data, (**b**) after background correction, and (**c**) after removing spikes, and normalizing. F_t: total DNR fluorescent intensity; F_b: background level; F_i: intracellular DNR fluorescent intensity; F_e: extracellular DNR fluorescent intensity

a *Raw data*

b *After smoothing and background correction ($F_i = F_t - F_b$)*

c *After removing spikes, and normalizing ($F_n = F_i / F_e$)*
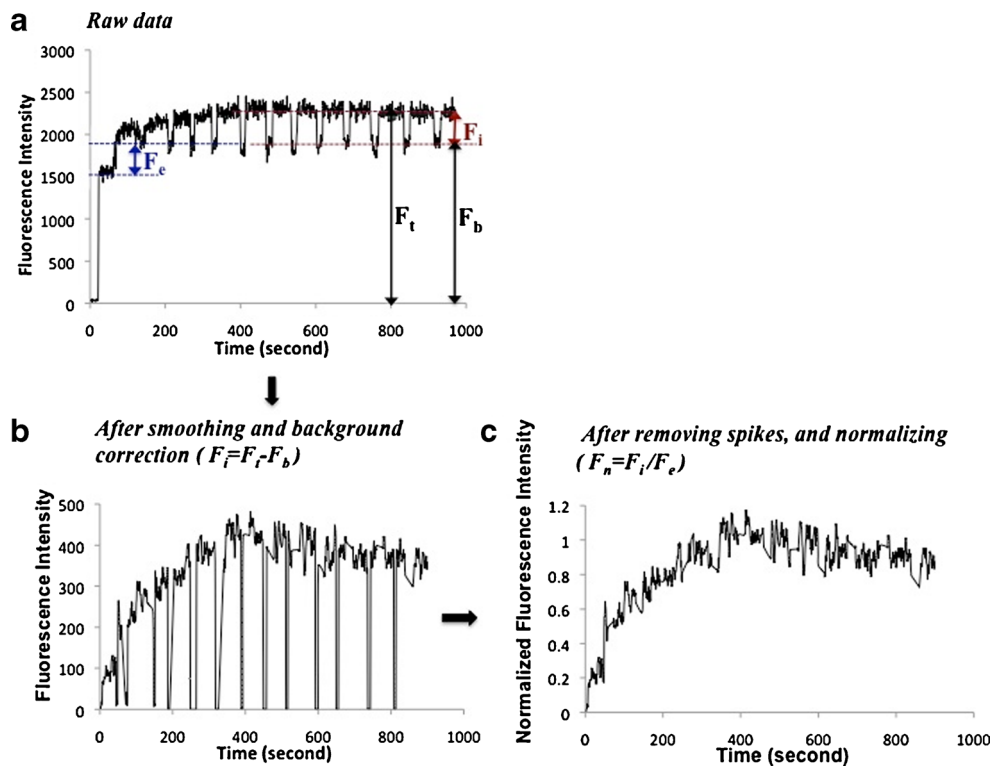
in drug accumulation was obtained when the DNR solution containing PCL5 was applied to the cell after 1000 s. The effectiveness of efflux blocking by this MDR inhibitor (PCL5) is indicated by the fold increase, which is defined as the ratio between the fluorescence signal of the inhibitor-blocked cell (treated by DNR in the presence of PCL5) and the fluorescence signal of the unblocked cell (treated by only DNR).

As shown in Fig. 4a, adding different concentrations of PCL5 (0.02 % w/v and 0.05 % w/v) notably increased drug accumulation and caused the single cell fluorescence to increase by 2.5- and 3.1-fold, respectively, in comparison to the DNR-only control ($P<0.0001$). No further fold increase was observed at a higher concentration (i.e., 0.1 % w/v, of PCL5). These values are comparable to, if not better than, the previously reported value of 1.3-fold [17].

The optical detection system allowed bright-field imaging and fluorescent measurement to be conducted simultaneously on a single cell isolated in a microfluidic chip, as previously described [40, 23]. In this regard, we were able to examine the cell morphological change attributable to DNR treatment during the *SASCA-A* experiment. Figure 4b shows the morphologies of this MDR cell before the experiment (using bright field observation), during experiment (simultaneous red light observation during fluorescence measurement) as treated by DNR drug, followed by adding DNR in the presence of PCL5, and after adding trypan blue. This dye was used to check if the cell membrane was compromised after the experiments, as a measure of cell viability (i.e., dead cells were stained in blue whereas the live cells remained unstained). As shown in
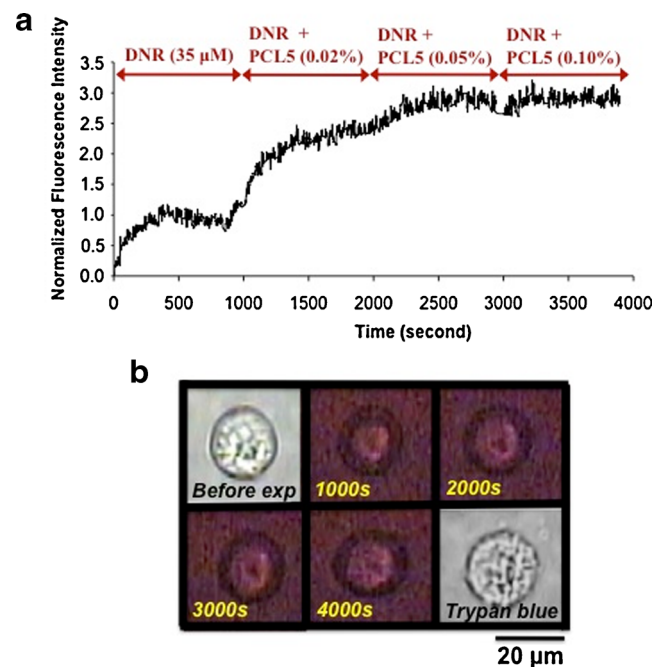

Fig. 4 (**a**) Drug accumulation on a single MDCKII-MDR1 cell in the presence of PCL5 as a P-gp inhibitor. The fold increase after adding different concentrations of PCL5 (0.02 %, 0.05 %, and 0.10 % w/v) was 2.5, 3.1, 3.1, respectively ($P<0.0001$). (**b**) The images of morphological change were shown before doing experiment, after treating the cell with DNR (1000 s), and after treating the cell with DNR plus PCL5 (2000, 3000, 4000 s), followed by adding trypan blue to check the cell viability. Scale bar: 20 μm

Fig. 4b, the cell was not stained by trypan blue, meaning that the SASCA measurement did not compromise the cell membrane permeability. In this experiment, although the cell membrane could be altered after adding PCL5, this cell membrane's integrity was preserved because no cell staining was observed after adding trypan blue.

More experiments were performed on single MDR and non-MDR cells in order to overcome the issue of cellular variations (see ESM Table S1 and S3, respectively). Applying only DNR to multiple single MDCKII-MDR1 cells resulted in low initial drug accumulations, but by treating the single cells with DNR in the presence of PCL5, the drug accumulations were increased (Fig. 5a, black column). The use of 0.02 %, 0.05 %, and 0.10 % w/v of PCL5 produced the averaged fold increases of 2.5 ± 0.2, 3.2 ± 0.3, and 3.2 ± 0.3, respectively ($n=3$). These were significant increases with the P values less than 0.01.

On the other hand, the *SASCA-A* measurement allows us to perform the fold-increase determination by directly using the drug accumulation data of one single cell. As shown in Fig. 5b (black column), the increase of drug accumulation in one single MDR cell after PCL5 addition is statistically significant

($P<0.0001$). This P-value is smaller in comparison to the one obtained from the averaged result of multiple single cells (see Electronic Supplementary Material for more results).

Similarly, experiments were conducted on MDCKII-MDR1 cells by using CsA as a positive P-gp inhibitor control. As shown in Electronic Supplementary Material, there were 1.4 ± 0.2 and 2.0 ± 0.2 fold increase in DNR accumulation in the presence of CsA of 2.5 μM and 5 μM ($P<0.01$), respectively, compared with the uninhibited cells (see ESM Table S4). As shown in Fig. 5c, in the single MDCKII-MDR cell treated only with 35-μM DNR (negative control), no significant fold increase was observed ($P>0.1$).

Conversely, conducting the same procedure on the wild type MDCKII cell did not result in substantial fluorescence enhancement as observed on the MDR cell. As shown in the hatched column in Fig. 5b, the initial fluorescent signals in the MDCKII cells were higher than those in the MDR cells, but observed fold was not high when the same cell was treated with DNR in the presence of different concentration of MDR inhibitors (1.2 ± 0.1, 1.3 ± 0.1, and 1.4 ± 0.1 fold increase for 0.02 %, 0.05 %, and 0.1%w/v of PCL5, respectively).
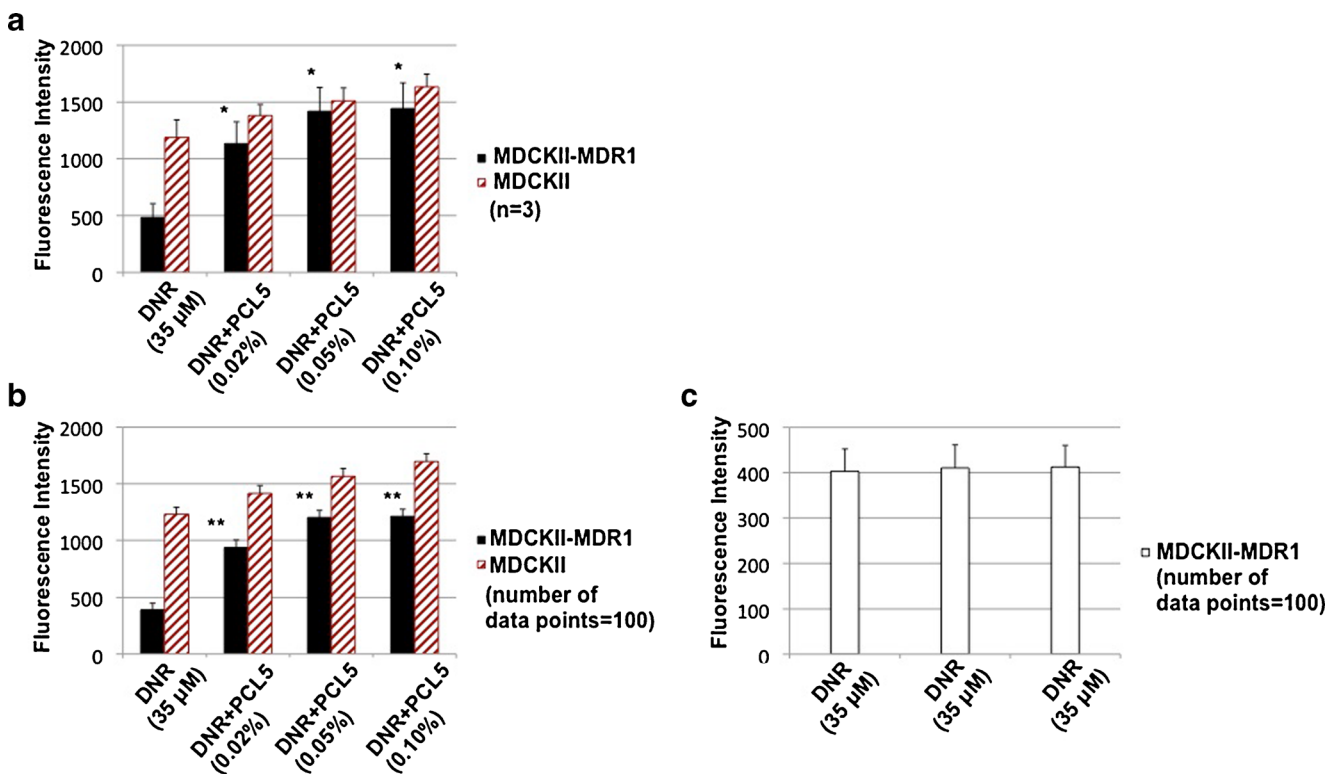

Fig. 5 Enhancement of DNR (35 μM) accumulation in MDCKII-MDR1 (black column) and MDCKII (hatched red column) cells by adding different concentration of PCL5 (0.02 %, 0.05 %, and 0.10 % w/v). (**a**) The fold increase after adding different concentrations of PCL5 on multiple MDR cells (black column) was 2.5 ± 0.2, 3.2 ± 0.3, and 3.2 ± 0.3, respectively. When DNR plus the same concentrations of PCL5 (0.02 %, 0.05 %, 0.10 % w/v) were applied on wild type MDCKII cells (hatched red column), the fold increase was not high (1.2 ± 0.1, 1.3 ± 0.1, and 1.4 ± 0.1 fold increase, respectively). *Indicates statistical significance ($P<0.01$). (**b**) The results of a single MDR and non-MDR cell (number of points: 100) were shown to compare with the above averaged results. The fold increase after treating the single MDR cell (black column) with the above concentrations of PCL5 was 2.4, 3.1, 3.1, respectively) (** $P<0.0001$). Similar experiment was performed on a single non-MDR cell (hatched column). No significant fold increase was observed (i.e., 1.1, 1.3, 1.4, respectively). (**c**) No significant fold increase was observed ($P>0.1$) in the single MDCKII-MDR cells (white column) treated in multiple times with 35-μM DNR only (negative control)
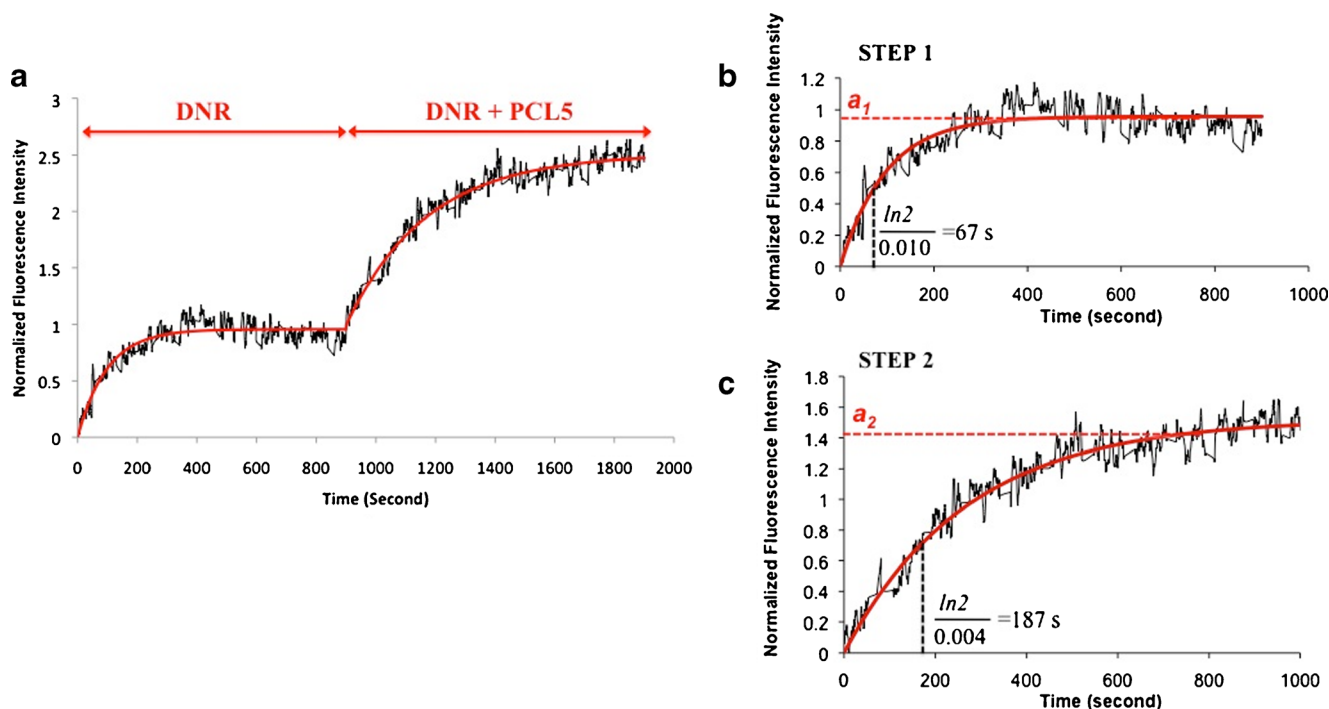
Fig. 6 Drug accumulation on the same single MDCKII-MDR1 cell in the absence and presence of PCL5 (0.02 % w/v) (**a**). Curve fitting was performed on step 1 (**b**) and step 2 (**c**) before inserting the fitted curves back to the overall data curve in (**a**). The black and red lines show raw data and curve fitting, respectively

In comparison to the conventional method, the *SASCA-A* method was capable of confirming the MDR reversal effect of PCL5 in a short time (~1 h) compared with drug accumulation measurements based on a 3-h microtiter plate-based assay [17]. For instance, Elamanchili et al. measured drug accumulation in PCL5/DOX-treated MDCKII-MDR1 cells compared with doxorubicin (DOX)-treated ones after 0–3 h of incubation [17]. These experiments were difficult and time-consuming to conduct using conventional methods, since they required many samples (12 samples for the 6 time points of DOX-treated cells in the absence and presence of PCL5), and several steps (0–3 h drug incubation, cell washing, and cell lysing before measurements of the released drug content using a scintillation counter). Even so, they reported just a 1.3-fold greater DOX accumulation in cells treated by 0.05 % w/v of PCL5 plus DOX in comparison to those cells treated with DOX alone [17].

Single cell drug accumulation kinetics and curve fitting

To better understand the drug accumulation kinetics in MDR cells, we applied a mono-exponential drug uptake model to fit the experimental *SASCA-A* data [41]. The following equation was used to describe the time-course change of single-cell DNR accumulation:

$$y = a\left(1 - e^{-bx}\right) \tag{3}$$

where x is the time; y is the ratio between intracellular and extracellular DNR concentrations (as described in Fig. 3a about data normalization); a is the value that y will reach when the time x is sufficiently large (this value is called pre-exponential factor that is related to the cell permeability coefficient p of drug uptake and the pump rate k for drug efflux [42]; b is the exponential factor which is the sum of p and k (the half time when y reaches 50 % of a is given by $\frac{\ln 2}{b}$) [41].

The curve fitting analysis was performed on the normalized DNR accumulation data, using SigmaPlot (ver. 11.0). The analysis was applied to the data obtained in the absence and presence of PCL5, as shown in Fig. 6, which depicts the data of only DNR accumulation (step 1), and data of drug accumulation enhanced by 0.02 % w/v of PCL5 (step 2). For the purpose of curve fitting, the data of step 1 and step 2 were separated, as shown in Fig. 6b and c, respectively; the two fitted curves were then combined in Fig. 6a. Because of the initially large drug concentration gradient, the initial drug accumulation rate is fast [42], and this is shown as a half time

Table 1 Curve fitting data to show drug accumulation of DNR (35 μM) in the same single MDCKII-MDR1 cell enhanced by PCL5 (0.02 % w/v)

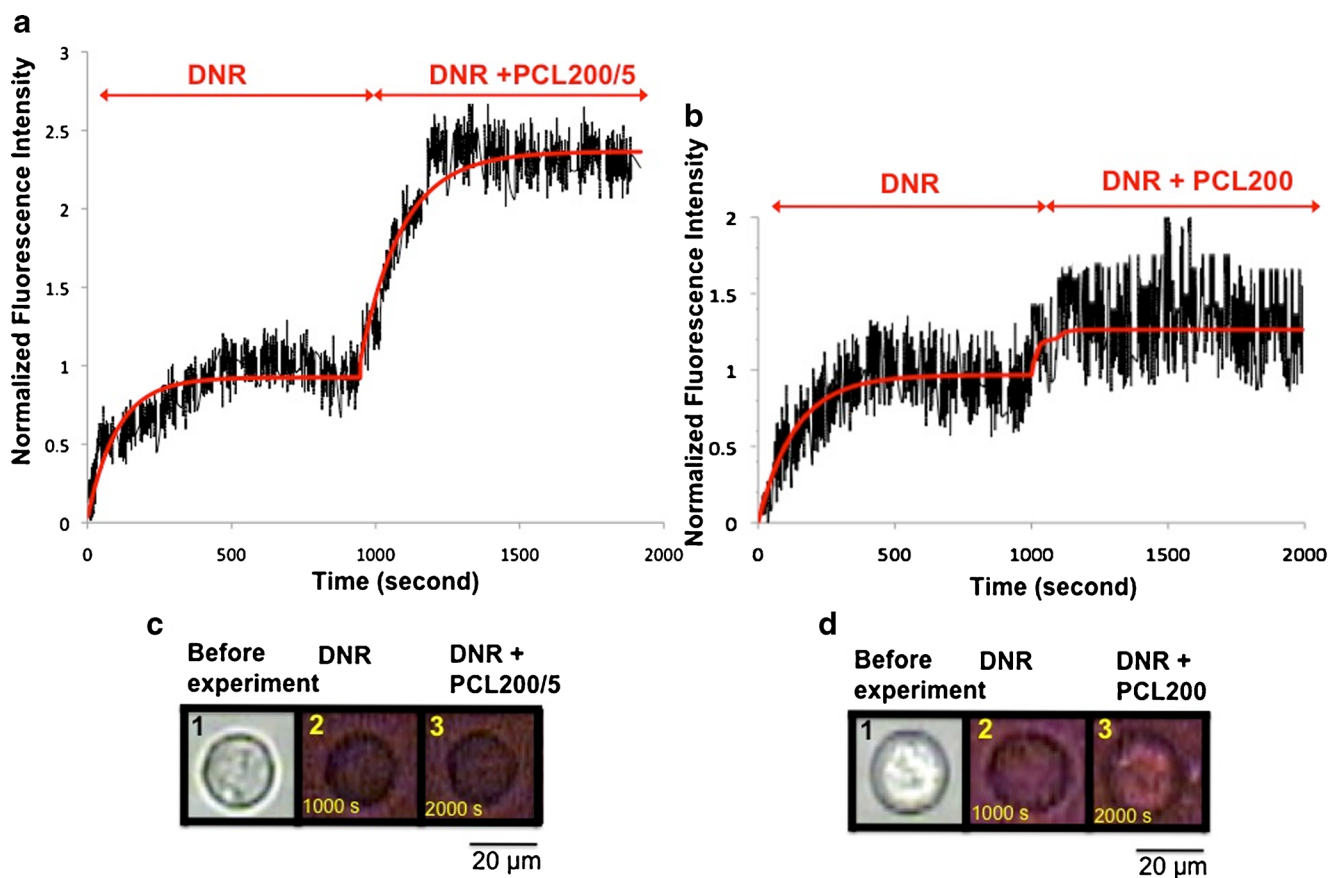| Step 1: DNR R^2=0.943 (n=900)		Step 2: DNR+PCL5 R^2=0.954 (n=880)	
a_1	b_1 (s^{-1})	a_2	b_2 (s^{-1})
0.95±0.12	0.010±0.006	1.42±0.22	0.004±0.002

Fig. 7 Effect of PCL200 on the drug accumulation on the MDCKII-MDR1 cell. Drug accumulation data are shown on one single cell in the presence of 0.02 % w/v of PCL200/5 (**a**) and on another single cell in the presence of 0.02 % w/v of PCL200 (**b**). The morphological changes of these cells before and after treatment with DNR (35 μM) in the presence of PCL200/5 (**c1**, **2**) and PCL200 (**d1**, **2**) were illustrated. As depicted, some aggregates surrounded the cell and attached to the cell membrane after PCL200 was applied to the cell. Those aggregates were not observed after treating the cell with PCL200/5. Scale bar: 20 μm

of ~ 67 s in Fig. 6b. When the concentration gradient across the cell membrane became smaller, the drug uptake rate became slower; ultimately, the signal reached a plateau as the drug uptake rate was close to the drug efflux rate. In the presence of PCL5, drug accumulation increased further (Fig. 6c), and it is believed to be caused by the action of PCL5 on the P-gp drug efflux pump. The curve fitting result is shown in Table 1. It was found that a increased from 0.95 to 0.95+1.42; b decreased from 0.010 to 0.004 s^{-1}, so the half time to reach the plateau increased from 67 to 187 s.

The fold increase could be calculated from the a values by adding 0.95 to 1.42 and dividing the sum by 0.95. Based on this calculation, a 2.6-fold increase (P<0.01) was obtained after treating the cell with DNR in the presence of PCL5. For

the b value in the absence and presence of PCL5, a 2.8-fold (P<0.01) change resulted. From the single-cell kinetic parameters, we could justify the fold increase of 2.5 (P<0.01) as obtained by our previous method (Fig. 4).

Effect of PCL200-encapsulated PCL5 on DNR accumulation

Since PCL5 has been shown to have an enhancement effect on DNR accumulation in MDR cells by inhibiting P-gp, this diblock copolymer will be a useful P-gp inhibitor for MDR tumors. Although DNR plus PCL5 are useful, encapsulation of this drug formulation (i.e., DNR + PCL5) is needed to achieve the appropriate controlled release in the context of chemotherapy. It is postulated that such an encapsulation can

Table 2 Curve fitting data to compare drug enhancement from PCL200/5 (0.02 % w/v) in MDCKII-MDR1 cells. DNR concentration was 35 μM

Step 1: DNR R^2=0.946 (n=890)		Step 2: DNR +PCL200/5 R^2=0.956 (n=880)	
a_1	b_1 (s^{-1})	a_2	b_2 (s^{-1})
0.97±0.22	0.016±0.006	1.36±0.20	0.007±0.006

Table 3 DNR accumulation enhancement in MDCKII-MDR1 cells by adding PCL200/5 (0.02 %, 0.05 %, 0.1 % w/v) and PCL5 (0.02 %, 0.05 %, 0.1 % w/v). The results were compared with drug accumulation in non-MDR cells. The statistical analysis of data was performed by the t-test (n=3)

Cell type	Treatment by DNR (35 μM) plus P-gp inhibitors	Mean fluorescent intensity	SD	t	P
MDCKII-MDR1	0	483.44	119.66		
	PCL 5 (0.02 %)	1133.50	192.65	4.96	0.007
	PCL 5 (0.05 %)	1419.38	207.14	6.78	0.002
	PCL 5 (0.10 %)	1443.42	224.00	6.55	0.002
MDCKII-MDR1	0	656.04	132.15		
	PCL 200/5 (0.02 %)	1598.63	202.64	7.05	0.003
	PCL 200/5 (0.05 %)	1927.91	212.99	9.15	0.001
	PCL 200/5 (0.10 %)	1793.44	233.51	7.60	0.002
MDCKII (Wild type)	0	1188.04	154.33		
	PCL 5 (0.02 %)	1381.81	97.77	1.84	0.140
	PCL 5 (0.05 %)	1511.72	111.35	2.95	0.050
	PCL 5 (0.10 %)	1633.08	111.19	4.05	0.020

be achieved by a copolymer of a longer diblock length such as MePEG$_{114}$-b-PCL$_{200}$ (PCL200), which takes the form of nanoparticles. In this regard, a similar *SASCA-A* experiment was done on this new drug formulation (i.e., PCL200/5 + DNR) to ensure that the enhancement effect of PCL5 was at least preserved, if not increased further. Although the mechanism of drug accumulation for these drug-loaded nanoparticles is not entirely clear, numerous research articles have described that the drug uptake likely occurs by engulfing the nanoparticles through endocytosis or by the partitioning of the drug through the cell membrane, or a combination of both [21, 43].

SASCA-A experiments on single MDCKII-MDR1 cells were conducted by using DNR (35 μM) mixed with PCL200/5 of different concentrations (0.02 %, 0.05 %, 0.1 % w/v). This nanoparticle system consists of PCL200 that encapsulates both a cytotoxic drug DNR and a polymeric P-gp inhibitor PCL5.

Drug accumulation experiments were conducted on two single MDCKII-MDR1 cells: one treated with PCL200/5 and the other one with PCL200, and a curve-fitting analysis was applied to the data. Figure 7a shows the cell treated with DNR in the absence and presence of PCL200-encapsulated PCL5 (PCL200/5). The normalized data is depicted in black and the result of the curve-fitting analysis is illustrated by the red line. At the very beginning, drug accumulation was fast for the first ~180 s. Thereafter, the drug uptake becomes slower until it reaches a steady state. From the curve fitting results shown in Table 2, it can be seen after applying PCL200/5, the b value decreased from 0.016 to 0.007 s^{-1}, resulting in a 2.4-fold decrease (P<0.01); based on the a values, a 2.4-fold increase was also obtained. Figure 7b shows the fitted curve of another single MDR cell, which was treated with DNR in the absence and presence of PCL200, showing no significant fold increase attributable to adding PCL200 nanoparticles alone.

The microfluidic method also allowed cell observation to be made during measurement; showing important changes such as cell morphology and undesirable aggregation of diblock copolymer nanoparticles. From the cell image in Fig. 7d-3, some particles were observed around the cell after PCL200 treatment. These particles, not seen before adding PCL200, are believed to be some aggregates formed from the unstable PCL200 nanoparticles. After mixing PCL5 with PCL200 as soon as it was synthesized, no aggregates were found to attach to the cell membrane (see Fig. 7c-3), PCL200 appeared to be stabilized by PCL5, and the new PCL200/5 formulation was shown to retain the MDR reversal property of PCL5.

More experiments were performed to confirm the MDR reversal effect of PCL200/5 on DNR accumulation in MDCKII-MDR1 single cells. As indicated in Table 3, when different concentrations of PCL200/5 (0.02 %, 0.05 %, 0.10 % w/v) were applied, a fold increase of DNR accumulation enhancement was observed. A high fold increase was observed when 0.05 % w/v of PCL200/5 was used. Since this
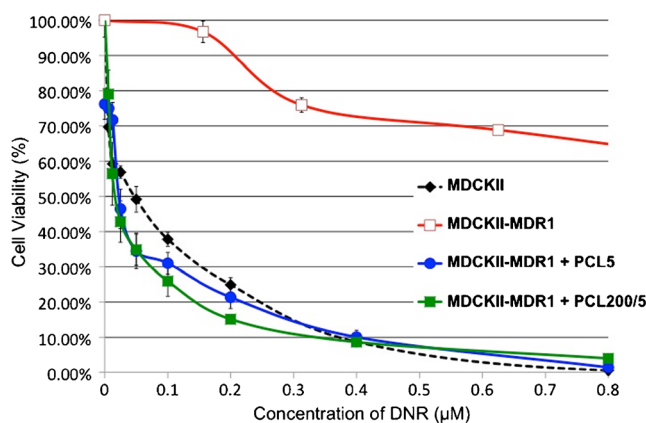

Fig. 8 The effect of DNR on MDCKII-MDR1 cell viability in the absence and presence of PCL5 (●) and PCL200/5 (0.05 % w/v) (■). The cytotoxicity of DNR in the absence and presence of PCL5 and the presence of PCL200/5 were shown in red, blue, and green lines, respectively. The black dashed line indicates the effect of DNR on MDCKII (wild type) cell viability. Notes: The cell viability was determined by an MTS assay. The values are the means of three independent experiments (±standard error of mean)

enhancement by PCL200/5 in DNR accumulation (P=0.001) is comparable to that by non-capsulated of PCL5 (P=0.002) in the same concentration of 0.05 % w/v, this result indicates that the effect of enhancement of DNR accumulation by PCL5 is retained after encapsulation in PCL200 nanoparticles. Data analysis conducted directly on each single MDR cell resulted in even lower P-values, obtained from treating the cells with PCL5 (Table S1 in the ESM) or with PCL200/5 (Table S2 in the ESM), thus confirming that there was significant enhancement in DNR accumulation by both drug formulations.

MTS cytotoxicity assays

The conventional method to examine the MDR reversal effect of an inhibitor compound is by using the MTS cytotoxicity assay. Although previous experiments (data not included) did not show the same results of DNR cytotoxicity in the PCL200-encapsulated PCL5 treatment as obtained from the un-encapsulated PCL5 treatment, this MTS assay was now repeated after the DNR accumulation enhancement of PCL200/5 was confirmed by *SASCA-A* experiment. Figure 8 indicates the cytotoxicity results of MDCKII-MDR1 cells in the presence of PCL5 and PCL200-encapsulated PCL5 (PCL200/5). Experiments were conducted to determine the cytotoxicity of the free anti-cancer drug for both MDCKII cells and MDCKII-MDR1 cells. Figure 8 shows that the MDR cells (red line) were much more resistant to DNR compared with wild-type MDCKII cells (black dashed line). Thereafter, we examined the cytotoxicity of DNR-loaded PCL5 at the most effective concentration (0.05 % w/v) on MDCKII-MDR1 cells. As shown in Fig. 8 (blue line), DNR-loaded PCL5 was capable of effectively reducing cell growth of MDR cells after 3 day incubation. Figure 8 (green line) indicates the results for PCL200/5 to be similar to PCL5. We should emphasize that the MDR reversal effect of PCL200/5 was only observed after changing its formulation (i.e., by mixing PCL200 with PCL5 as soon as PCL200 was synthesized).

Conclusion

Consistent with previously reported results using conventional methods, the greatest drug accumulation was achieved using 0.05 % w/v of PCL5 as determined by the *SASCA-A* method. Although the actual mechanism of how encapsulated PCL5 increased drug accumulation remains unknown, the enhancement of drug accumulation occurred quickly without delay, and so it is believed that PCL5 was released from the nanoparticle carrier promptly. When PCL5 is encapsulated in PCL200, it has been reported that the diblock copolymers of two molecular weights are associated because of the hydrophobic interaction between the PCL blocks [17]. It is hypothesized that some unimers of PCL5, which are in dynamic equilibrium with those

associated with the nanoparticles [44], interact with the cell membrane and change its membrane fluidity [45, 46], leading to P-gp inhibition. Because an incubation time of 3 d is needed for a cytotoxicity assay and 3 h for a radiochemical drug accumulation assay, this hypothesis cannot be easily verified. Since the *SASCA-A* experiment is completed in a short period of time, our results indicate the ability of PCL5 to enhance drug accumulation is fast; therefore, it can be inferred that the association of PCL5 unimers with the PCL200 nanoparticles might be loose and so PCL5 is quickly released to inhibit the P-gp activity and enhance the drug accumulation in MDR cells. By using *SASCA-A*, we were able to confirm that encapsulated PCL5 in the formulation of PCL200/5 had the same P-gp inhibitory activity as the un-encapsulated PCL5. This important finding suggests that PCL5 co-administered with the DNR-loaded nanoparticle can be used to overcome the drug efflux effect in cancer cells. In addition to fast analysis, *SASCA-A* only requires a small number of cells and drugs to confirm the response to P-gp inhibitors; therefore, this technique may be potentially useful for investigating the MDR effect with minimal cell requirements and for assisting patients undergoing chemotherapy in the future.

References

1. Thomas H, Coley HM (2003) Overcoming multidrug resistance in cancer: an update on the clinical strategy of inhibiting p-glycoprotein. Cancer Control 10(2):159–165
2. Chan LMS, Lowes S, Hirst BH (2004) The ABCs of drug transport in intestine and liver: efflux proteins limiting drug absorption and bioavailability. Eur J Pharm Sci 21:25–51
3. Marquez B, Van Bambek F (2011) ABC multidrug transporters: target for modulation of drug pharmacokinetics and drug–drug interactions. Curr Drug Targets 12:600–620
4. Sharom FJ (2008) ABC multidrug transporters: structure, function, and role in chemoresistance. Pharmacogenomics 9(1):105–127
5. Ayesh S, Shao YM, Stein WD (1996) Cooperative, competitive, and noncompetitive interactions between modulators of P-glycoprotein. Biochim Biophys Acta 1316(1):8–18
6. Shaffer BC, Gillet JP, Patel C, Baerc MR, Batesa SE, Gottesman MM (2012) Drug resistance: still a daunting challenge to the successful treatment of AML. Drug Resist Updat 15:62–69
7. Seeling A, Gerebtzoff G (2006) Enhancement of drug absorption by noncharged detergents through membrane and P-glycoprotein binding. Expert Opin Drug Metab Toxicol 2(5):733–752
8. Zhang W, Shi Y, Chen Y, Ye J, Sha X, Fang X (2011) Multifunctional pluronic P123/F127 mixed polymeric micelles loaded with paclitaxel for the treatment of multidrug resistant tumors. Biomaterials 32(11): 2894–2906

9. Sachs-Barrable K, Thamboo A, Lee SD, Wasan KM (2007) Lipid excipients peceol and gelucire 44/14 decrease P-glycoprotein mediated efflux of rhodamine 123 partially due to modifying P-glycoprotein protein expression within Caco-2 cells. J Pharm Pharmaceut Sci 10(3):319–331

10. Bogman K, Erne-Brand F, Alsenz J, Drewe J (2003) The role of surfactants in the reversal of active transport mediated by multidrug resistance proteins. J Pharm Sci 92(6):1250–1261

11. Brittner B, Guenzi A, Fullhardt P, Zuercher G, Gonzalez RC, Mountfield RJ (2002) Improvement of the bioavailability of colchicine in rats by co-administration of D-α-tocopherol polyethylene glycol 1000 succinate and a polyethoxylated derivative of 12-hydroxy-stearic acid. Arzneim-Forsch Drug Res 52(9):684–688

12. Letchford K, Zastre J, Liggins R, Burt H (2004) Synthesis and micellar characterization of short block length methoxy poly(ethylene glycol)-block-poly(caprolactone) diblock copolymers. Colloids Surf B Biointerfaces 35(2):81–91

13. Hugger ED, Novak BL, Burton PS, Audus KL, Borchardt RT (2002) A comparison of commonly used polyethoxylated pharmaceutical excipients on their ability to inhibit P-glycoprotein activity in vitro. J Pharm Sci 91(9):1991–2002

14. Rege BD, Kao JP, Polli JE (2002) Effects of nonionic surfactants on membrane transporters in Caco-2 cell monolayers. Eur J Pharm Sci 16(4/5):237–246

15. Woodcock DM, Linsenmeyer ME, Chojnowski G (1992) Reversal of multidrug resistance by surfactants. Br J Cancer 66(1):62–68

16. Wan CPL, Letchford K, Jackson JK, Burt HM (2013) The combined use of paclitaxel-loaded nanoparticles with a low-molecular-weight copolymer inhibitor of P-glycoprotein to overcome drug resistance. Int J Nanomed 8:379–391

17. Elamanchili P, McEachern C, Burt HM (2009) Reversal of multidrug resistance by methoxypolyethylene glycol-block-polycaprolactone diblock copolymers through the inhibition of P-glycoprotein function. J Pharm Sci 98(3):945–958

18. Zastre J, Jackson JK, Wong W, Burt HM (2007) Methoxypolyethylene glycol-block-polycaprolactone diblock copolymers reduce P-glycoprotein efflux in the absence of a membrane fluidization effect while stimulating P-glycoprotein ATPase activity. J Pharmaceut Sci 96(4):864–875

19. Zastre J, Jackson JK, Burt HM (2004) Evidence for modulation of P-glycoprotein-mediated efflux by methoxypolyethylene glycol-block-polycaprolactone amphiphilic diblock copolymers. Pharmaceut Res 21(8):1489–1497

20. Zastre J, Jackson J, Bajwa M, Liggins R, Iqbal F, Burt HM (2002) Enhanced cellular accumulation of a P-glycoprotein substrate, rhodamine-123, by Caco-2 cells using low molecular weight methoxypolyethylene glycol-block-polycaprolactone diblock copolymers. Eur J Pharm Biopharm 54(3):299–309

21. Letchford K, Liggins R, Wasan KM, Burt H (2009) In vitro human plasma distribution of nanoparticulate paclitaxel is dependent on the physicochemical properties of poly(ethylene glycol)-block-poly(caprolactone) nanoparticles. Eur J Pharm Biopharm 71(2):196–206

22. Wan L, Letchford K, Leung D, Jackson J, and Burt HM (2014) Mixed Molecular Weight Copolymer Nanoparticles for the Treatment of Drug Resistant Tumors: Formulation Development and Cytotoxicity. Journal of Pharmaceutical Sciences (Manuscript id: 14–539.R1)

23. Li X, Ling V, Li PCH (2008) Same-single-cell analysis for the study of drug efflux modulation of multidrug resistant cells using a microfluidic chip. Anal Chem 80(11):4095–4102

24. Di Carlo D, Lee LP (2006) Dynamic single-cell analysis for quantitative biology. Anal Chem 78(23):7918–7925

25. Li X, Huang J, Tibbits GF, Li PCH (2007) Real-time monitoring of intracellular calcium dynamic mobilization of a single cardiomyocyte

26. Gu SQ, Zhang YX, Zhu Y, Du W, Fang Q (2011) Multifunctional picoliter droplet manipulation platform and its application in single cell analysis. Anal Chem 83(19):7570–7576

27. Li X, Chen Y, Li PCH (2011) A simple and fast microfluidic approach of same-single-cell analysis (SASCA) for the study of multidrug resistance modulation in cancer cells. Lab Chip 11(7):1378–1384

28. Peng XY, Li PCH (2004) A three-dimensional flow control concept for single-cell experiments on a microchip. 1. Cell selection, cell retention, cell culture, cell balancing, and cell scanning. Anal Chem 76(18):5273–5281

29. Shen F, Li XJ, Li PCH (2014) Study of flow behaviors on single-cell manipulation and shear stress reduction in microfluidic chips using CFD simulations. Biomicrofluidics 8(014109):1–12

30. Wang Z, Pal D, Patel A, Kwatra D, Mitra AK (2013) Influence of overexpression of efflux proteins on the function and gene expression of endogenous peptide transporters in MDR-transfected MDCKII cell lines. Int J Pharmaceut 441:40–49

31. Wan CPL, Jackson JK, Pirmoradi FP, Chiao M, Burt HM (2012) Increased accumulation and retention of micellar paclitaxel in drug-sensitive and P-Glycoprotein-expressing cell lines following ultrasound exposure. Ultrasound Med Biol 38(5):736–744

32. Agarwal S, Pal D, Mitra AK (2007) Both P-gp and MRP2 mediate transport of lopinavir, a protease inhibitor. Int J Pharm 339:139–147

33. Xiao Y, Davidson R, Smith A, Pereira D, Zhao S, Soglia J, Gebhard D, de Morais S, Duignan DB (2006) A 96-well efflux assay to identify ABCG2 substrates using a stably transfected MDCK II cell line. Mol Pharm 3:45–54

34. Wang Q, Rager JD, Weinstein K, Kardos PS, Dobson GL, Li J, Hidalgo IJ (2005) Evaluation of the MDR-MDCK cell line as a permeability screen for the blood–brain barrier. Int J Pharm 288:349–359

35. Tang F, Horie K, Borchardt RT (2002) Are MDCK cells transfected with the human MDR1 gene a good model of the human intestinal mucosa? Pharm Res 19:765–772

36. Li X, Li PCH (2005) Microfluidic selection and retention of a single cardiac myocyte, on-chip dye loading, cell contraction by chemical stimulation, and quantitative fluorescent analysis of intracellular calcium. Anal Chem 77(14):4315–4322

37. Peng XY, Li PCH (2005) Extraction of pure cellular fluorescence by cell scanning in a single-cell microchip. Lab Chip 5(11):1298–1302

38. Horio M, Chin KV, Currier SJ, Goldenberg S, Williams C, Pastan I (1989) Transepithelial transport of drugs by the multidrug transporter in cultured Madin-Darby canine kidney cell epithelia. J Biol Chem 264:14880–14884

39. Qadir M, O'Loughlin KL, Fricke SM, Williamson NA, Greco WR, Minderman H, Baer MR (2005) Cyclosporine A is a broad-spectrum multidrug resistance modulator. Clin Cancer Res 11(6):2320–2326

40. Li XJ, Xiaoyan X, Li PCH (2009) Real-time detection of the early event of cytotoxicity of herbal ingredients on single leukemia cells studied in a microfluidic biochip. Integr Biol 1:90–98

41. Stein WD (1997) Kinetics of the multidrug transporter (P-glycoprptein) and its reversal. Physiol Rev 77(2):545–590

42. Collander R (1954) The permeability of Nitella cells to nonelectrolytes. Physiol Plant 7:420–445

43. Zastre JA, Jackson JK, Wong W, Burt HM (2008) P-glycoprotein efflux inhibition by amphiphilic diblock copolymers: relationship between copolymer concentration and substrate hydrophobicity. Mol Pharm 5(4):643–653

44. Letchford K, Burt H (2007) A review of the formation and classification of amphiphilic block copolymer nanoparticulate structures: micelles, nanospheres, nanocapsules, and polymersomes. Eur J Pharm Biopharm 65:259–269

in a microfluidic chip pertaining to drug discovery. Electrophoresis 28(24):723–4733

45. Kabanov AV, Batrakova EV, Alakhov VY (2003) An essential relationship between ATP depletion and chemosensitizing activity of pluronic block copolymers. J Control Release 91(1/2):75–83

46. Collnot EM, Baldes C, Schaefer UF, Edgar KJ, Wempe MF, Lehr CM (2010) Vitamin E TPGS P-glycoprotein inhibition mechanism: influence on conformational flexibility, intracellular ATP levels, and role of time and site of access. Mol Pharm 7(3):642–651

47. Li PCH (2006) Microfluidic Lab-On-A-Chip for Chemical and Biological Analysis and Discovery. Taylor and Francis Group, CRC, New York